PERGAMON

International Journal of Heat and Mass Transfer 42 (1999) 3195–3204

International Journal of HEAT and MASS TRANSFER

Estimation of thermal effects in cavitation of thermosensible liquids

Daniel H. Fruman[a,*], Jean-Luc Reboud[b,1], Benoît Stutz[b,2]

[a]*Ecole Nationale Supérieure de Techniques Avancées, Groupe Phénomènes d'Interface (GPI), 91761 Palaiseau Cedex, France*
[b]*Laboratoire des Ecoulements Géophysiques et Industriels, Institut de Mécanique de Grenoble (LEGI-IMG), B.P. 53, 38041 Grenoble Cedex 9, France*

Received 16 October 1997; received in revised form 16 December 1998

Abstract

Vapour production through cavitation extracts heat from the fluid surrounding the cavity and creates a temperature difference between liquid and vapour. This thermal effect is particularly significant in cryogenic liquids. Estimates of the temperature difference can be made provided: (a) the rate of vapour production required to sustain a given cavity, and (b) and appropriate model for the heat exchange at the interface of the cavity are known. The vapour production is usually estimated by assuming that it is equal to the non-condensable gas flow rates necessary to sustain ventilated cavities of equal geometry. It has been shown that experimental results previously obtained can be quite satisfactorily predicted if the interface is assimilated to a rough flat plate through which the amount of heat necessary to generate the vapour is being fed. In order to obtain data for cavities developed over walls whose geometry and pressure gradient are analogous to those of turbopump inducers, and to achieve a better precision, tests were conducted in a specially designed cavitation loop operating with R-114. It is shown that the experimental results are well predicted by the proposed model.

1. Introduction

Vapour production through cavitation extracts heat from the fluid surrounding the cavity and creates a temperature gradient between the free stream liquid temperature and the interface of the vapour cavity. The difference of temperature between the liquid and the vapour constitutes what is usually named the thermal effect and is particularly significant in cryogenic liquids such as those utilized in the turbopumps of the European space launcher Ariane. In order to determine the temperature difference, tests are conducted with thermosensible fluids, often other than those employed in the prototype applications, using, generally, small-scale models and measuring the temperature within the cavity using thermocouples installed on the wall of the test objects. Once the scale and thermosensible fluid test results are known, the question is how to extrapolate the temperature differences to the prototype situations.

The earlier procedure consisted in defining a non-dimensional temperature difference number, *B*-factor [1], and to correlate it as a function of powers of other non-dimensional parameters characterizing the scale, the flow conditions and the fluid characteristics [2,3].

* Corresponding author. Present address: 16, allée Bellevue, 78230 Le Pecq, France.
[1] Present address: Ecole Nationale d'Ingénieurs de Saint Etienne, 58, rue J. Parot, 48023 Saint Etienne Cedex 2, France
[2] Laboratoire de Thermodynamique et Energetique, Université de Pau, av. de l'Université, 64000 Pau, France

0017-9310/99/$ - see front matter
PII: S0017-9310(99)00005-8

Nomenclature

B	non-dimensional temperature difference
b	cavity width
C	foil chord
C_f	flat plate friction coefficient
c_p	specific heat at constant pressure
C_Q	flow coefficient
D	diameter of headforms
L	latent heat of vaporization
l	cavity length
Pr	Prandtl number
p_{ref}	reference upstream pressure in the venturi test section
p_v	vapour pressure
Q	vapour production or air injection flow rate
$Re_{x,l}$	Reynolds number computed with the distance $x(l)$
t	foil thickness
T_p	wall (interface) temperature
T_{ref}	reference temperature
T_w	temperature measured at the wall of the venturi test section
u_b	velocity at the edge of the viscous boundary layer
U_{ref}	reference velocity
U_∞	reference velocity in the venturi test section
V_g	mean velocity of the vapour (air) uniformly distributed over the cavity interface
x	distance along the flat plate (interface)
y	distance normal to the venturi wall
ΔT	temperature difference ($T_{ref}-T_p$)
ΔT_{visc}	increase of temperature due to viscous dissipation.

Greek symbols

α	void fraction
ϵ	roughness of the flat plate (interface)
φ_p	heat flux transferred to the flat plate (interface)
ρ	liquid specific mass
ρ_v	vapour specific mass
σ	cavitation number.

Subscripts

r	rough plate
s	smooth plate.

In order to improve the correlations, Holl et al. [3] introduced an additional non-dimensional number obtained using the flow rate of air, or of other non-condensable gas, necessary to produce a ventilated cavity of a given length on a geometrically similar body. This constituted the 'entrainment method'. It improved the correlations but was unable to estimate the thermal effect with enough accuracy for a variety of flow conditions. Therefore, these methods require the performance of two series of experiments: one in a thermosensible fluid in cavitation conditions and the other in non cavitating conditions with ventilated cavities filled with air or another non-condensable gas.

Brennen [4] set indirectly the basis of a predictive procedure when he investigated the air diffusion across the interface of a supercavitating cavity behind a spherical headform. He observed that a turbulent boundary layer on the cavity surface developed following the separation point on the headform surface, and demonstrated that this layer played the predominant role in the air diffusion process. He assumed that the momentum thickness of the boundary layer was constant along the interface, approximated by a flat surface, and extended his air diffusion model to the vapour flux through the interface as a function of the difference, ΔT, between the upstream, T_{ref}, and cavity

temperatures, T_c. By rearranging the expression given by Brennen, in order to have it in SI units and assuming that the laminar-to-turbulent boundary layer transition coincides with the separation point on the headform surface, ΔT is expressed by

$$\Delta T = T_{ref} - T_c = \frac{\rho_v L C_Q}{0.896 \rho c_p} \frac{1}{\sqrt{1+\sigma}} \sqrt{\frac{l}{\delta_2}} \quad (1)$$

where ρ and ρ_v are the specific mass of the liquid and the vapour respectively, L is the latent heat of vaporization, δ_2 is the momentum thickness of the boundary layer, c_p is the specific heat, C_Q is a volumetric flow coefficient,

$$C_Q = \frac{Q}{U_{ref} \pi D l} = \frac{V_g}{U_{ref}} \quad (2)$$

σ the cavitation number,

$$\sigma = \frac{p_{ref} - p_v(T_{ref})}{\frac{1}{2} \rho U_{ref}^2} \quad (3)$$

with Q the vapour flow rate, U_{ref} and p_{ref} the free stream velocity and pressure, l the length of the cavity, D the diameter of the headform, p_v and v the vapour pressure and the kinematic viscosity of the liquid.

In Eq. (2),

$$V_g = \frac{Q}{\pi D l} \quad (4)$$

is the velocity of the vapour supposedly being produced uniformly on the surface of the cavity.

If we replace δ_2 by its expression for a turbulent boundary layer on a smooth flat plate, (1) can be written as:

$$\Delta T = T_{ref} - T_c = \frac{\rho_v L C_Q}{0.17 \rho c_p} \frac{Re_l^{-0.1}}{\sqrt{1+\sigma}} \quad (5)$$

where Re is the Reynolds number,

$$Re_l = \frac{U_{ref} l}{v} \quad (6)$$

Equating the vapour flow rate to the air flow rate of a ventilated cavity of equal length, Brennen computed the temperature difference in the case of cold water and showed that it was minute. A major conclusion of Brennen's work was that the 'the volume rate of entrainment of all gas and vapour is dependent only on water speed and cavity size for steady cavities behind a particular headform', and that 'this result seems reasonable and may be true for all steady cavities' [4]. In fact, we will see later that the non-dimensional flow rate, expressed in the form given by Eq. (2), is—within the scattering due to experimental errors—constant whatever the shape of the headform or hydrofoil and regardless of whether partial or supercavitating conditions prevail.

Therefore, it seems possible to predict the thermal effect provided: (a) the rate of vapour production required to sustain a given cavity, and (b) an appropriate model for the heat exchange at the interface of the cavity are known. This approach has been promoted by Fruman et al. [5] and Fruman and Beuzelin [6], who proposed to assimilate the cavity interface to a rough flat plate without pressure gradient and the vapour production to the non-condensable gas flow rates necessary to sustain ventilated cavities of equal geometry and to determine the temperature deficit using the usual heat exchange formulations. In their approach, vapour is supposed to be produced uniformly on the cavity interface and no other source of vapour are considered to exist. The relative roughness of the interface is an unknown parameter and it was estimated by Fruman and Beuzelin [6] using the experimental results obtained by Hord with a hydrofoil in liquid hydrogen and nitrogen [7] and a venturi tube in liquid hydrogen [8]. Using a constant flow coefficient, obtained from ventilation tests conducted in two different geometries, the adjustment of the very numerous experimental results by Hord was quite satisfactory whatever the shape of the cavitating body and the flowing liquid provided the roughness was selected to be Reynolds number dependent.

To further substantiate these results and to insure that they could be used in the estimation of the thermal effect for cavities developed over walls whose geometry and pressure gradient are analogous to those of turbopump inducers, experimental results of tests, conducted in a specially designed cavitation loop operating with R-114 ($C_2Cl_2F_4$), developed with the support of the Agence Française de l'Espace (CNES) and the Société Européenne de Propulsion (SEP) and operated by the Centre de Recherches et d'Essais de Machines Hydrauliques de Grenoble (CREMHyG), were used. Tests consisted in measuring the temperature, the void fraction and the vapour production of R-114 cavities and comparing the latter with the air required to sustain a ventilated cavity of equal length using water as a flowing liquid.

This paper presents the results of these experiments and a comparison of the experimental temperature differences with those predicted using the Fruman et al. [5] approach. The predicted and measured temperature differences compare very favourably.

2. Experimental

The R-114 experimental facility (called Plateform

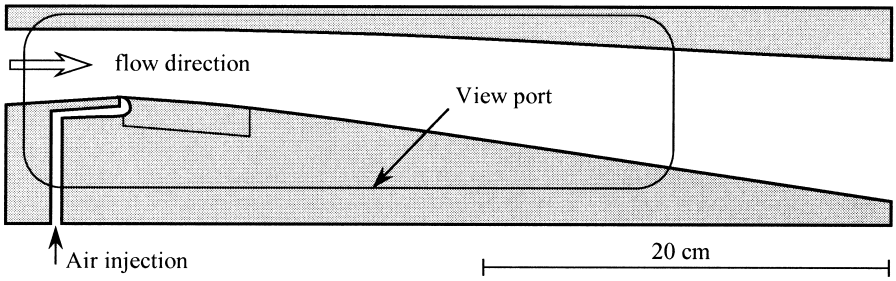

Fig. 1. Schematic of the venturi in the test facilities.

d'Essais de Cavitation de Liquides à Effet Thermodynamique (PECLET)) is a closed loop operating with a reference pressure, obtained by pressurizing, up to 35 bar, a reservoir with nitrogen gas. To prevent gas dissolution into the circulating liquid, a flexible membrane separates the liquid and gas phases. The loop is fitted with a test section having the shape of a two-dimensional venturi (Fig. 1 without the air injection slit), designed in such a way that the pressure distribution is analogous to the one existing on the upper surface of an inducer blade [9]. The lower wall of the venturi makes, upstream of the throat, an angle of -4.3° with the horizontal, while, downstream of the throat section, a divergent with an angle of 4° extends up to 250 mm. Beyond, the divergent angle increases to 8°. The upper wall is nearly horizontal up to a distance of 150 mm downstream of the throat, where an angle of 3.1° reduces the divergent aperture. The throat section is 44 mm in width and 43.7 mm in height and the velocity can be varied between 16 and 45 m/s. Temperature can be varied and controlled from 20 to 40°C. Under these experimental conditions, it is possible to achieve cavities having a maximum length of 12 cm before choking. Temperatures on the venturi plastic (PVC) wall next to the cavity were measured using five micro-thermocouples situated at 3, 20, 38, 75 and 115 mm from the throat. These wall temperatures are assumed to be those of the two phase fluid in contact with the wall and, by extension, those of the interface at the same axial station. One reference temperature was measured 20 cm upstream. Mean cavity interfaces were visualized with a video camera and the length determined by image processing [9].

A facility having the same test section as the R-114 loop was operated with water as a running fluid and pressurised by air. It allowed to conduct tests of ventilated cavities by performing air injections through a two-dimensional slit situated slightly downstream of the venturi throat, Fig. 1. The injected air (or non-condensable gas) is evacuated as a two-phase wake downstream of the cavity closure. The maximum velocity at the throat was only 20 m/s and the pressure was set in order to avoid vapour production at the ventilated cavity interface. The air flow rate was measured using either a turbine flow meter or a rotameter. The same loop was also used to perform vapour cavitation tests. Void fraction and phase velocity in the cavity were measured using specially designed optical probes [10,11]. Vapour and gas flow rates were obtained by integration of the void fraction and velocity profiles [12].

Cavitation will occur at the venturi throat when the local static pressure in there is equal to the vapour pressure, that is to say $\sigma_c = -C_{pmin}$. A potential flow calculation gives a $-C_{pmin}$ equal to 1.4. When the σ value is decreased below the critical value ($-C_{pmin}$), a sheet cavity is initiated at the sharp edge formed by the upstream convergent and downstream divergent and will develop on the lower surface of the venturi. For a cavity length of about 80 mm, the maximum thickness of the cavity is comprised between 6 and 7 mm. Therefore the radius of curvature of the interface, assumed to be fitted by an arc of a circle, will be about 300 mm. Under such circumstances, the height of the cavity is about 2% of the radius of curvature and the hypothesis of a flat plate seems to be then fully justified.

3. Proposed model

The vapour production is supposed to be given by the flow coefficient, Eq. (2), and, in order to generalize it, πD is made equal to the cavity width b. We will also assume that the flow is turbulent and that the surface behaves as a rough plate. The validity of the above assumptions can only be verified if the results are favourably compared with available data. This has been made first using Hord's data for a hydrofoil in liquid hydrogen and nitrogen and a venturi tube in liquid hydrogen and, in section 5, the comparisons will be extended to the R-114 tests.

Let us first consider the case of a turbulent flow on a smooth plate. It can be shown [13] that the wall temperature on a smooth flat plate over which a heat flux, φ_p, is being transferred by the fluid is given, for Prandtl numbers $Pr \approx 1$, by,

$$T_p = T_{ref} + \frac{\varphi_p}{\frac{1}{2}\rho c_p U_{ref} C_f}\left(1 - \frac{u_b}{U_{ref}}(1 - Pr)\right) \quad (7)$$

where C_f is the local friction coefficient, u_b is the velocity at the edge of the viscous boundary layer and

$$\varphi_p = -\rho_v L V_g = -\rho_v L C_Q U_{ref} \quad (8)$$

For a smooth plate, the ratio u_b/U_{ref} is given by [13]

$$\frac{u_b}{U_{ref}} = \frac{2.1}{Re_x^{0.1}} \quad (9)$$

which leads to

$$T_p = T_{ref} + \frac{\varphi_p}{\frac{1}{2}\rho c_p U_{ref} C_f}\left(1 - \frac{2.1}{Re_x^{0.1}}(1 - Pr)\right) \quad (10)$$

Now, according to [14], for a rough plate, the difference between the wall temperature and the reference temperature, $(T_p - T_{ref})_r$, is related to the one for a smooth plate, $(T_p - T_{ref})_s$, by

$$(T_p - T_{ref})_r = \eta \frac{(C_f)_s}{(C_f)_r}(T_p - T_{ref})_s \quad (11)$$

with $(T_p - T_{ref})_s$ being given by Eq. (10).

In Eq. (11), $(C_f)_s$ and $(C_f)_r$ are the local friction coefficients for a smooth and a rough plate respectively; η is a multiplying factor which is less or equal to 1 for the Prandtl's numbers and the roughness that are usually considered.

C_Q was obtained through ventilation tests during which air (or some other non-condensable gas) was injected through a slit situated slightly downstream the cavity and evacuated as a two-phase wake at the trailing edge of the cavity.

At very high Reynolds numbers, $(C_f)_r$ is expressed by

$$\frac{1}{2}(C_f)_r = 0.00695\left(\frac{x}{\epsilon}\right)^{-1/7} \quad (12)$$

where ϵ is the equivalent roughness.

Finally, under the assumption that $\eta \approx 1$, combining Eq. (11) to Eqs. (10) and (12), we obtain, for a turbulent flow on a rough plate,

$$T_p = T_{ref} - \frac{\rho_v L C_Q}{0.00695 \rho c_p}\left(\frac{x}{\epsilon}\right)^{1/7}[1 - 2.1 Re_x^{-0.1}(1 - Pr)] \quad (13)$$

In order to perform calculations with Eq. (13) it is necessary to know the value of C_Q and to have an estimate of ϵ.

From tests of ventilation conducted using a backward facing step and a hydrofoil having a flat upper surface, Fruman and Beuzelin [6] determined that the air flow rate required to sustain the cavities was a linear function of the free stream velocity and the cavity length. In other words, the flow coefficient defined by Eq. (2) was constant and independent of the geometry of the tested body with a mean value of 5.2×10^{-3}. It should be pointed out that ventilation tests were conducted by Yoshihara et al. [15], with a hydrofoil having the same shape as the one used by Hord. The authors gave a flow coefficient in the form of

$$C_Q^* = \frac{Q}{U_{ref} B t} = 7.66 \times 10^{-2}\left(\frac{l}{C}\right)^{0.88}$$

where t and C are respectively the thickness and the chord of the foil.

In the form given by Eq. (2) we have, taking into account that $C = 0.1$ m and $t/C = 0.06$, $C_Q = 3.49 \times 10^{-2} l^{-0.12}$, with l in meters. The dependence of the flow coefficient on the cavity length is very weak and, for cavity lengths between 1.7 and 5 cm, their values are between 5 and 5.7×10^{-3}, very close to the one obtained by Fruman and Beuzelin for cavities smaller than 8 cm. Also, the data obtained by Billet and Weir [16] for ventilation ogives of three diameters, 0.318, 0.635 and 1.27 cm, give a nearly constant flow coefficient, when the flow rate is reported to the exposed cavity interface surface, although the values are higher, by as much as a factor of 2, than those reported above. This particular behaviour of ventilated cavities seems to be quite universal since Brennen [4] in his tests with axisymmetric headforms has also shown that the volume rate of entrainment was dependent only on cavity size and tunnel velocity in spite of the fact that the length of the cavities he considered was of 0.50, 0.75 and 1.12 m, one order of magnitude larger than those investigated by Fruman and Beuzelin [6] and usually encountered in tests conducted by Hord. With the value of $C_Q = 5.2 \times 10^{-3}$, Fruman and Beuzelin estimated the apparent roughness by adjusting Hord's data for the hydrofoil in two cryogenic liquids [7] and for the venturi tube in liquid hydrogen [8]. The best adjustment was obtained by using a roughness (in meters), varying with the Reynolds number, of the form,

$$\epsilon = 2.2 Re_x^{-0.5} \quad (14)$$

For the Reynolds numbers of Hord's tests, the roughness is, in absolute terms, quite large, of the order of a millimeter, and can result, in physical terms, from the bumped characteristics of the cavity interface.

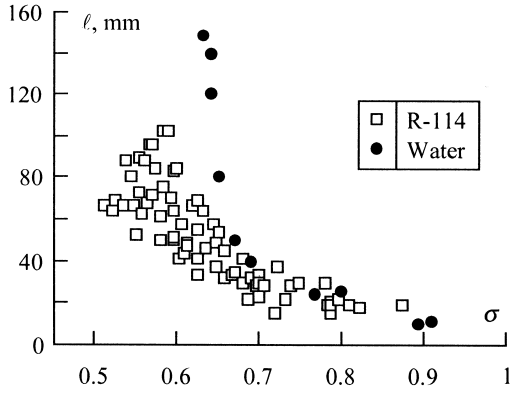

Fig. 2. Cavity length as a function of cavitation number in the PECLET and water facilities.

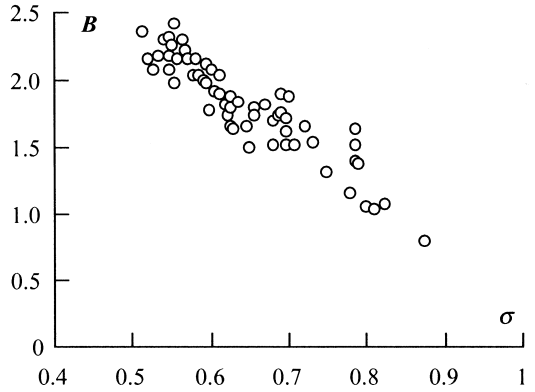

Fig. 4. B factor vs cavitation number.

4. Experimental results in R-114 and water loops

4.1. Thermal effect results

The length of the cavity has been plotted as a function of the cavitation number in Fig. 2 for tests performed in the PECLET and water loops. In the latter case the cavity length increases very sharply for σ values of less than 0.70 while in the case of R-114, the increase is less marked. The difference between the R-114 and the water results can be explained because of the thermal effect since the cavitation number computed with the temperature within the cavity would be larger than the one used in Fig. 2, and the difference will increase with the cavity length increasing.

Fig. 3 shows ΔT_w, the difference between the free stream temperature and the venturi wall temperature, as a function of the distance to the throat, non-dimensionalized with the cavity length (50 mm), for three reference temperatures and flow velocities. Temperatures decrease linearly with distance whatever the experimental conditions. The maximum values of ΔT_w for each test condition are presented as a non-dimensional coefficient B,

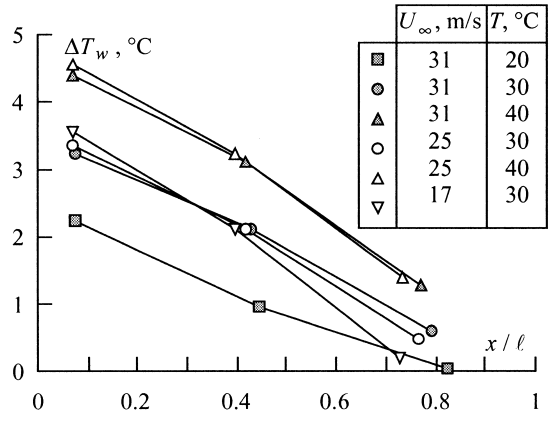

Fig. 3. Temperature difference as a function of distance to the throat for $l = 50$ mm.

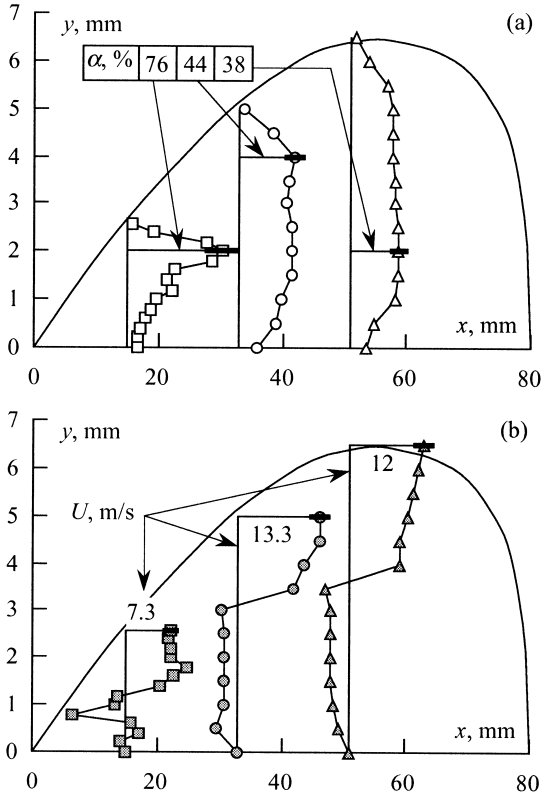

Fig. 5. Void fraction (a) and velocity (b) profiles at three stations for $U_\infty = 14$ m/s and a ventilated cavity length of 80 mm. (Notice that the vertical scale is 10 times the horizontal one.)

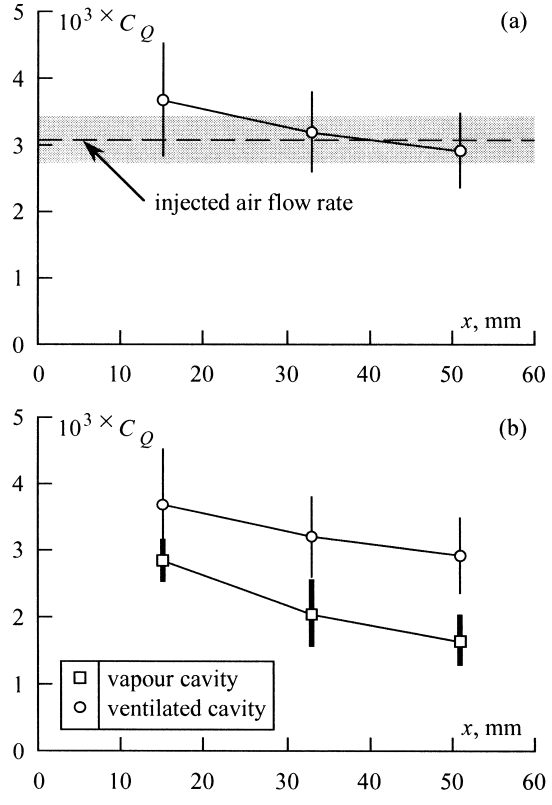

Fig. 6. Local flow coefficients obtained by integration of the product of the void fraction and the velocity from Figs. 5 and 7.

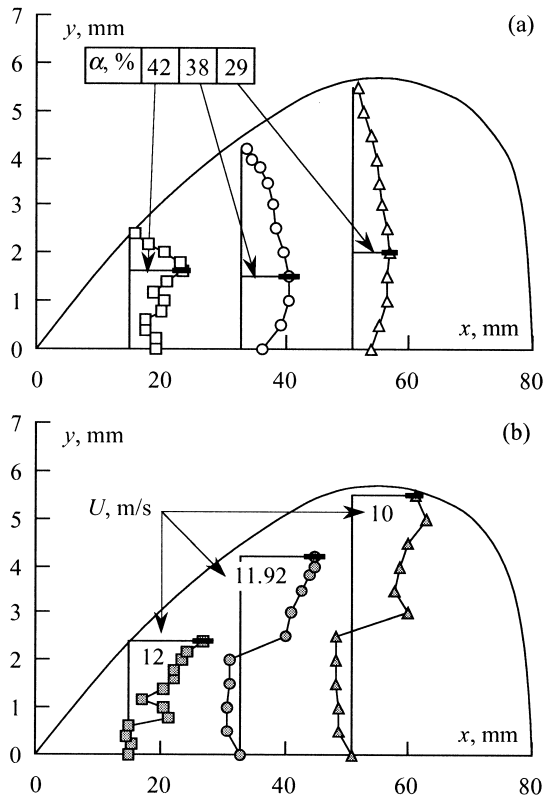

Fig. 7. Void fraction (a) and velocity (b) profiles at three stations for $U_\infty = 14$ m/s and a vapour cavity length of 80 mm. (Notice that the vertical scale is 10 times the horizontal one.)

$$B = (\Delta T_{\mathrm{wmax}})\frac{\rho c_{\mathrm{p}}}{\rho_{\mathrm{v}} L} \tag{15}$$

as a function of σ in Fig. 4. In spite of some inevitable experimental scattering, the data points are quite well correlated. In all these tests, ΔT_{wmax} is comprised between 1 and 5°C.

4.2. Flow coefficient for ventilated cavities

For the peculiar geometry of the venturi used in the tests, the flow coefficients and the Reynolds numbers were computed using, as a reference velocity, the velocity of the cavity interface given by the Bernoulli's Eq. $U_{\mathrm{ref}} = U_\infty(1+\sigma)^{1/2}$, where U_∞ is the velocity in the control section of the venturi. The mean flow coefficient is independent of Reynolds numbers (thus independent of velocity and cavity length) in the range tested, which is much smaller than those usually encountered in practical applications and in the PECLET loop. The value obtained is $C_Q = 3.1 \times 10^{-3} \pm 0.45 \times 10^{-3}$. The difference between this value and the one reported in Section 3 is mainly due to the selection of the reference velocity and, as it will be seen later, does not affect the final results. The scatter is principally associated to the precision of the measurement of the cavity length. It can be estimated to ±10% and is due essentially to the fluctuations of the cavity closure. Stutz [11], has conducted velocity and void fraction measurements within a 8 cm long ventilated cavity. He showed, Fig. 5a, that near the leading edge of the cavity the void fraction peaks at the interface while becoming nearly constant over the cavity height downstream. The velocities are in the direction of the main flow on the upper half of the cavity thickness and show a backflow in the lower half, Fig. 5b. This backflow justifies the homogenization of the void fraction by the intense mixing so created. The air (vapour) flow rate was computed by integrating, over the cavity thickness at different stations, the product of the velocity and the void fraction. In spite of the difficulties associated with this type of measurements and the precision of the integration, conducted with a limited number of data points, the comparison with the injected air flow rate is very much satisfactory, Fig. 6a.

4.3. Flow coefficient for vapour cavities

For the geometry of the venturi used in the ventilation tests, Stutz [11] performed velocity and void fraction measurements for an 8 cm long natural stable cavity, Fig. 7. As compared to the ventilated cavity situation, the void fraction does not show a significant augmentation near the leading edge in the vicinity of the interface. Further downstream, the void fraction is larger near the wall than near the interface. The velocity profiles are surprisingly close to the ones of the ventilated cavity. In terms of vapour flow coefficients, Fig. 6b shows that they are slightly below the non-condensable gas flow coefficients but close enough to justify a posteriori the hypothesis of the entrainment theory [3]. The difference may be associated to some unaccounted condensation effects in the vapour cavity.

For unsteady nearly periodic cavities, Larrarte [17] has shown that the vapour production can be assimilated to the cavity growth rate during the initial phase. Assuming that there is no vapour production during the phase of cavity detachment and cloud convection, the mean vapour flow rate during the total duration time of a period gives a flow coefficient 4–6 times larger than the one of the stable cavity. However, Stutz and Reboud [10] have shown that the mean void fraction of these cavities during the growth phase is around 20%. If this void fraction is taken into account, the vapour flow coefficient is reduced (by a factor of about 5) and the flow coefficient estimates are then close to the ones for stable cavities.

4.4. Preliminary conclusions

The results presented above show that the hypothesis of the entrainment theory, which assumes that the vapour flow rate can be estimated by the non-condensable gas flow rate required to sustain a ventilated cavity, are quite well justified by the experiments if due account is taken of the difficulty of conducting very precise measurements in vapour cavities. The methodology developed by Fruman and co-workers to estimate the thermal effect will now be applied to the flow conditions of the PECLET loop tests.

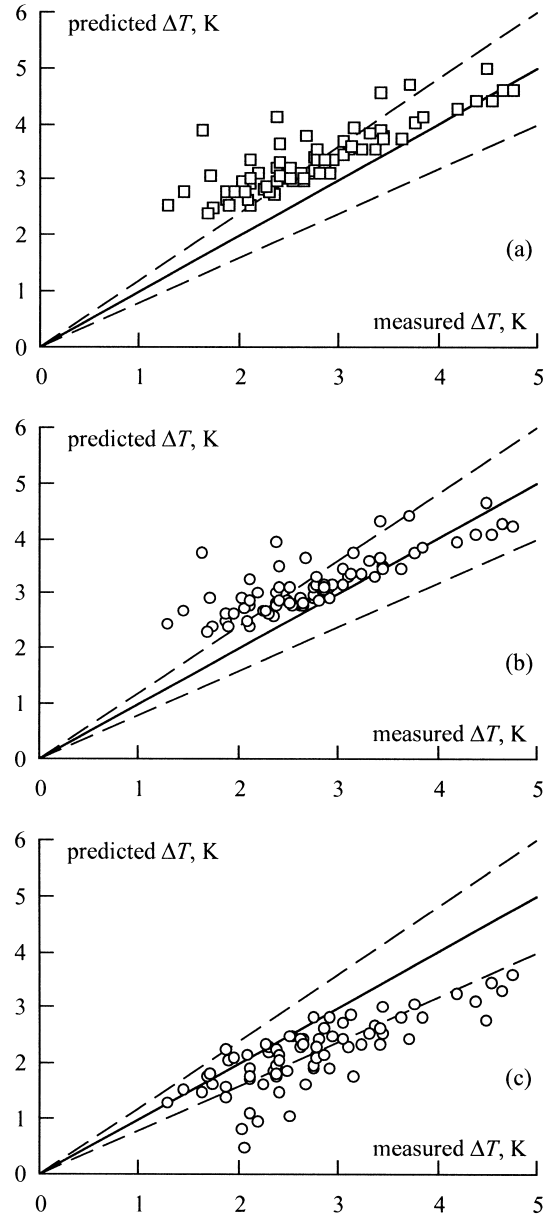

Fig. 8. Predicted vs measured temperature difference for (a) values of the parameters at the free stream temperature, (b) values of the parameters for the vapour phase at the temperature computed using the temperature difference given in (a), and (c) including viscous heating effect.

5. Comparison of experimental and predicted temperature differences

For prediction purposes it is preferable to use data obtained in simple test conditions and with unsophisticated instrumentation. This is the case for the flow coefficient in ventilated conditions. Thus, the C_Q given in Section 4.2 and Eqs. (13) and (14) for $x=l$, are used to estimate the temperature differences. The results, computed using the characteristics of the liquid and vapour phases at the reference conditions, are shown in Fig. 8a as a function of the experimental ΔT together with the straight lines corresponding to the slope unity (continuous) and $\pm 20\%$ difference (discontinuous). It can be seen that the predicted values of ΔT are larger than the experimental ones, in particular for moderate ΔT (<3 K). For the $\Delta T > 3.5$ K, they are

well within the ±20% margin. Among the many factors which can justify these differences, a screening investigation has shown that the vapour phase characteristic parameters in Eq. (13), calculated for the reference temperatures instead of the cavity temperatures, are the most significant. Indeed, using the characteristics of the vapour phase for the temperature in the cavity obtained from the previous computation, the estimated ΔT are slightly reduced, but remain too large in the moderate ΔT range, Fig. 8b. Moreover, because of the high velocities of the liquid flow (20 m/s < U_{ref} < 50 m/s), the heat produced by viscous effects might not be neglected. According to Eckert and Drake [14], in the case of turbulent boundary layers the increase of temperature induced by viscous effects can be estimated (from experiments) by,

$$\Delta T_{visc} = \frac{U_{ref}^2}{2c_p} Pr^{1/3} \tag{16}$$

The ΔT_{visc} given by Eq. (16) was then subtracted from the data points shown in Fig. 8b to account for viscous heating. The results are plotted in Fig. 8c. Here, the predictions became reasonable for most of the data in the moderate ΔT range but slightly underestimated beyond $\Delta T \approx 3$ K.

These results are, in any event, very satisfactory taking into account that no predictive method is today available and that tentative numerical modelling of this complex problem has failed to provide for good temperature differences estimates. They give an a posteriori justification to the heat transfer assumptions, rough flat plate without pressure gradient, sustaining the model. However, the heat production by viscous effects is probably not as significant as Eq. (16) predicts, and the assumption that the vapour production is uniformly distributed over the whole cavity interface may not be fully justified (based on the results presented in Fig. 6, showing that the flow coefficient has reached its maximum value at the first measuring station downstream the cavity leading edge). Moreover, the size of the adopted equivalent roughness cannot be justified either on physical grounds and has to be considered as an adjustable parameter whose physical meaning is yet to be found.

6. Conclusion

Results of tests conducted in two cavitation loops having the same geometric venturi type test section are presented. In one of the test loops the working fluid is R-114 and allows us to determine the temperature reduction due to the vapour produced to feed a natural cavity. In the other loop, operating with water, tests were conducted with ventilated and natural stable cavities to determine the non-condensable gas and vapour production rates by performing void fraction and velocity measurements within the cavities.

A model is presented that allows the computation of the temperature reduction by assuming that: (i) the vapour production is equal to the air injection necessary to sustain a ventilated cavity of equal mean length; (ii) the vapour production is uniformly distributed on the whole surface of the cavity interface, and (iii) the interface behaves as a rough flat plate through which heat is fed to produce the vapour.

The experimental results show that the hypothesis of equality between gas flow rate and vapour production rate is rather well justified. Comparison between the experimental temperature differences (liquid/interface) and the values obtained using the proposed model show that reasonable estimates can be made, taking into account the precision of the measurements of (a) the cavity length, (b) the air flow rate and (c) the simplicity of the model. Use of the liquid properties at the free stream conditions and the vapour properties at the interface temperature, resulting from the first computation at the reference conditions, improves the results. If the temperature augmentation produced by viscous dissipation is taken into account, the temperature differences due to vapour production are reduced. The experimental temperature differences are well within the extreme values calculated for the reference temperature and with the correction for viscous heating.

Since no method of prediction of the temperature difference in thermosensible fluids is available today, the suggested method can be considered as highly reliable in spite of its limitations. Work needs to be conducted in order to improve the accuracy of the measurements of the length of the cavities, in particular for highly unstable situations, and of the air (or non-condensable gas) flow rate in ventilated cavities, as well as to interpret the significance of the equivalent roughness.

Acknowledgements

The authors acknowledge the financial support of the Agence Française de l'Espace (CNES) and express their gratitude to Dr G. Albano for his continuous interest on this project. The design, construction and operation of the PECLET facility was made possible thanks to funds and engineering assistance provided by the Société Européenne de Propulsion (SEP).

References

[1] H.A. Stahl, A.J. Stepanoff, Thermodynamics aspects of

cavitation in centrifugal pumps, Trans. ASME. J. Basic. Eng. 87 (1956) 309.

[2] R.D. Moore, R.S. Ruggeri Prediction of thermodynamic effects on developed cavitation based on liquid hydrogen and Freon 114 data in scaled venturis, NASA TN D-4899, 1969.

[3] J.W. Holl, M.L. Billet, D.S. Weir, Thermodynamic effect on developed cavitation, J. Fluids Eng. 97 (1975) 507.

[4] C. Brennen, The dynamic balance of dissolved air and heat in natural cavity flows, J. Fluid Mech. 37 (1975) 115.

[5] D.H. Fruman, I. Benmansour, R. Sery, Estimation of the thermal effects on cavitation of cryogenic liquids, Cavitation and Multiphase Flow Forum, ASME FED 109 (1991) 93–96.

[6] D.H. Fruman, F. Beuzelin, Effets thermiques dans la cavitation des fluides cryogéniques, La Houille Blanche 7/8 (1992) 557–561.

[7] J. Hord, Cavitation in Liquid Cryogens, Volume II—Hydrofoil, NASA CR-2156, 1973.

[8] J. Hord, L.M. Anderson, W.J. Hall, Cavitation in liquid cryogens: Venturi, NASA CR-2054, 1972.

[9] J.L. Kueny, J.L. Reboud, J. Desclaux, Analysis of partial cavitation: image processing and numerical prediction, Cavitation '91, ASME-FED 116 (1991) 55–60.

[10] B. Stutz, J.L. Reboud, Experiments on unsteady cavitation, Experiments in fluids 22 (1997) 191–197.

[11] B. Stutz Analyse de la structure diphasique et instationnaire de poches de cavitation. Doctoral Thesis, INP Grenoble, France 1996.

[12] B. Stutz, J.L. Reboud, Two phase flow structure of sheet cavitation, Physics of Fluids 9 (12) (1997) 3678–3686.

[13] E.A. Brun, A. Martinot-Lagarde, J. Mathieu, Mécanique des Fluides 3, Dunod, Paris, 1970.

[14] E.R.G. Eckert, R.M. Drake, Analysis of Heat and Mass Transfer, McGraw-Hill Book Co, 1972.

[15] K. Yoshihara, H. Kato, H. Yamaguchi, M. Miyanaga, Experimental study on the internal flow of a sheet cavity, Cavitation and Multiphase Flow Forum, ASME-FED 64 (1988) 94–98.

[16] M.L. Billet, D.S. Weir, The effect of gas diffusion on the flow coefficient for a ventilated cavity, J. Fluids Eng. 97 (1975) 501.

[17] F. Larrarte, A. Pauchet, P. Bousquet, D.H. Fruman, On the morphology of natural and ventilated cavities, Cavitation and Multiphase Flow Forum, ASME-FED 210 (1995) 31–38.